J Mol Model (2014) 20:2501
DOI 10.1007/s00894-014-2501-4

ORIGINAL PAPER

Emulating structural stability of *Pseudomonas mendocina* lipase: *in silico* mutagenesis and molecular dynamics studies

Parameswaran Saravanan · Vikash Kumar Dubey · Sanjukta Patra

Received: 22 July 2014 / Accepted: 13 October 2014 / Published online: 1 November 2014

Abstract The need of alkaline detergent-stable lipases has been growing rapidly as they are highly attractive for the production of detergents, biodiesel, pharmaceuticals agents, and various other applications. Lipase from *Pseudomonas mendocina* (PML) is one such candidate with triglyceride activity and non-homologous with other reported *Pseudomonas* lipases. The present work provides insights on the role of amino acids toward structural stability of PML. PML was subjected to mutagenesis through *in silico* point mutations for emulating its structural stability, the foremost property to enhance biophysiochemical properties for industrial process. The structural effects of identified mutants on PML have been analyzed through comparative atomistic molecular dynamics simulations on wild type and mutants. The *in silico* mutants P187A and P219A were found to stabilize their respective local dynamics and improved the structural stability of PML. The current study sheds light on the rational engineering of PML through *in silico* methodologies to improvise its structural stability as well as prototype for rational engineering of the lipases.

Keywords Lipase · Molecular dynamics · Point mutation · *Pseudomonas mendocina* · Rational engineering · Stability · 3D structure

Electronic supplementary material The online version of this article (doi:10.1007/s00894-014-2501-4) contains supplementary material, which is available to authorized users.

P. Saravanan · V. K. Dubey · S. Patra (✉)
Department of Biotechnology, Indian Institute of Technology Guwahati, Guwahati 781039, Assam, India
e-mail: sanjukta@iitg.ernet.in

Introduction

Lipases are attractive biocatalysts for food, dairy, organic synthesis, pharmaceuticals, oleochemical, paper, leather, and detergent industries [1–5]. Their applicability gets wider when they possess thermostability, organic solvent stability, substrate specificity, chemo-, regio-, and enantio-specific behavior [6, 7]. However, there is need to engineer lipases toward such stability factors [8–10]. In this direction, checking all possible mutations through experimental approaches is time and resource intensive [11]. Detailed understanding of the three dimensional (3D) structure of lipases would aid in rationally engineering them to function in the desired industrial environments [12–14]. Therefore, *in silico* rational approach is useful to select optimistic mutations that could be validated experimentally [15]. The present work is an attempt in this direction.

The need of alkaline detergent-stable lipases has been growing rapidly owing to their industrial applications [16]. Detergent industry is the primary consumer of lipases [17]. Totally 21 lipases have been reported to have application in the detergent industry while 43 lipases have been reported as alkaline (maximum pH greater than or equal to 9) in Brenda enzyme database [18]. New and improved lipases with appropriate properties for industrial process are in continuous demand in detergent industry and for novel applications [19]. To attain any such individual or multitude of such properties, enhancement of stability of the protein is the foremost step. Apart from high activity and stability, alkaline detergent-stable lipases should have compatibility with the detergent components in washing conditions including surfactants, oxidants, solvents, and other enzymes [19–21]. *Pseudomonas mendocina* lipase (PML) is such a lipase which has been reported as a potential fat stain remover [22, 23]. PML has α/β hydrolase fold with conserved catalytic triad Ser126,

His206, and Asp176. It is active in its monomer form with pH range of 8 to 10 and its 3D structure is non-homologous from other reported *Pseudomonas* lipases. PML does not require metal ions and interfacial activation for its optimum activity making it a unique attractive industrial biocatalyst.

The availability of PML structure (PDB Id: 2FX5) facilitates bioinformatics studies for rational engineering intended to make PML more robust with improved performance, industrial applicability and storage. The *in silico* mutagenesis were carried out to identify structurally important amino acids for identifying mutagenesis hotspots prone to mutation by any possible amino acids. Proteins stability were investigated between wild type and identified mutants of PML with the help of molecular dynamics (MD) simulations. Identification of mutagenesis hot spots and mutants with enhanced structural stability will be instrumental in understanding and making PML, a commercially viable lipase.

Material and methods

The current study implements a rational approach to emulate structural stability of PML utilizing its 3D experimental structure. Structurally/strategically residues were identified for understanding structural stability of PML. The mutagenesis hotspots were predicted followed by the identification of *in silico* mutants. The *in silico* mutants were analyzed and validated with MD simulations utilizing well established parameters to understand the structural changes induced by the mutation.

Prediction of *in silico* mutants

PML was investigated for the stability prediction upon point mutation with ProSA (prosa2003 program) [24]. The methodology was explained in detail in our previous work on *Staphylococcus aureus* lipase [25]. The experimental structure of PML (PDB Id: 2FX5) was utilized for the prediction of *in silico* mutants. ProSA reflects the quality of all possible mutations on each residue using knowledge-based potentials. The predicted mutations were classified as stabilizing and destabilizing mutations based on z-scores which aids us to identify the mutagenesis hotspots of PML.

MD simulations to identify 'thermolabile' residues

To identify dynamic 'thermolabile' residues, a 20 ns MD simulation was performed in an explicit water environment with the periodic boundary conditions applied in three dimensions using GROMACS package [26–28]. The net charge of system was neutralized by the addition of counter ions by replacing water molecules that are at least 3.50 angstroms (Å) from the protein surface. The solvent was equilibrated for 100 ps by restraining the solute atoms through a harmonic force constant of 1000 kJ mol^{-1} nm^{-2} in NVT ensemble followed by NPT ensemble. NPT production run was carried out for 20 ns with no restraints using 2 fs of integration time. All MD simulations were carried out with temperature of 300 K with velocity rescaling thermostat in which protein and non-protein atoms were coupled to separate temperature coupling baths. The pressure was controlled at 1 atm using Parrinello-Rahman barostat. The particle mesh Ewald (PME) summation method was used for calculating the long-range electrostatic interactions with cut-off of 12 Å. The linear constraint solver (LINCS) algorithm was used to constrain the bonds involving hydrogen atoms [26]. The dynamic residues were based on root-mean square fluctuations (RMSF) that can be correlated to temperature factors which reflects the local structural flexibility. The mutants were selected based on the presence of 'thermolabile' residues.

Validation of identified *in silico* mutants through MD simulations

The identified *in silico* mutants were studied in detail to provide insight at the atomic level with the help of 20 ns MD simulations with the optimized parameters of PML. The comparative MD analysis between the mutants and wild type identify potential mutants with better structural stability. MD trajectories were analyzed with built-in Gromacs tools. The root-mean square deviation (RMSD) and RMSF of the backbone carbon atoms were studied with g_rmsd and g_rmsf respectively to understand the degree of conformational changes in the respective 3D structures of the candidate lipases and mutants. The secondary structure analysis was carried out using the Kabsch and Sander algorithm incorporated in their Dictionary of Secondary Structure for Proteins (DSSP) program [29] which was installed into Gromacs to analyze the variation of protein secondary structure changes. Program g_gyrate was used to measure the radius of gyration which reflects the compactness of the structure. Program g_sas was used to compute interaction surface areas between solvent molecules and complexes. Sigmaplot was utilized to prepare the plots of trajectory analysis from MD simulations and the figures were produced using Adobe PhotoShop.

Results and discussion

In silico Mutagenesis of PML

PML is an attractive fat stain remover for industrial applications [22, 23]. To check the change in overall structural stability of PML, point mutation was carried out on each residue using ProSA [24, 25]. Based on *in silico* mutagenesis,

we identified four sets of residues which might lead to destabilization of structure of PML. In the first set, 24 positions were predicted at which substitution of any 1 of these 24 positions by the rest of the 19 amino acids will lead to destabilization of the protein (class 1). The second set is comprised of 15 positions which can be mutated by 1 corresponding amino acid without affecting the protein stability (class 2). Similarly, set 3 and 4 are comprised of 26 and 32 positions respectively which can be mutated by 2 and 3 corresponding residue without affecting the protein stability (class 3 and class 4). The four class identified 97 amino acid residues as structurally/strategically important for PML which were distributed throughout the protein. Furthermore, five residues Pro7, Pro10, Glu83, Pro187, and Pro219 were identified as stabilizing mutants where substitution by any other amino acid does not affect the structural stability of PML and herein referred as mutagenesis hotspots (Fig. 1). Based on the RMSF data from MD simulation of PML, 'dynamic residues' with local disorderedness/structural flexibility were identified as Arg91, Arg163, and Gln242. The mutagenesis hotspots and thermolabile dynamic residues were identified as *in silico* mutants of PML (Table 1).

Validation of *in silico* mutagenesis with molecular dynamics

Sibille *et al.* demonstrated that the MD simulation of PML were strikingly similar to that of experimental data (^{15}N relaxation and H/D exchange rates) and proved MD as a versatile tool to identify and study mutants to improve the structural stability [23]. The *in silico* mutants identified from ProSA and RMSF study were investigated with the wild type of PML through atomistic MD simulations. The mutants were chosen based on the biophysical principles to improve their respective secondary structure. Proline being helix breaker, it is well documented that mutating proline into alanine in α-helix would improvise the structural stability through improvised hydrogen bonds [30]. Mutation of a residue into proline in the loop region contributes to increased structural and proteolytic stability in proteins which is proven in *Bacillus subtilis* lipase and *Pseudomonas glumae* lipase [31, 32]. The identified mutants were validated with comparative MD simulations of wild type and mutants to increase the structural stability of PML were listed in Table 2.

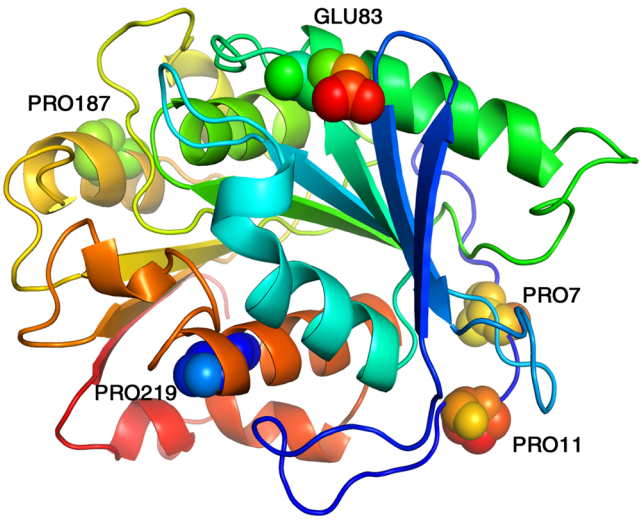

Fig. 1 Mutagenesis hotspots with stabilizing mutants of PML

Table 1 List of thermolabile dynamic residues based on the RMSF data of PML

Residues	Secondary structure*
R91A	α-helix
R163P	loop
Q242P	loop

* the secondary structure where thermolabile 'dynamic' amino acids resides

Root mean square deviation (RMSD) The degree of conformational changes of wild type and mutants of PML was monitored by root mean square deviation of α-carbon atom during the course of molecular dynamics simulation. The backbone RMSD of conformations from production run relative to its initial structure has been studied and represented in Figs. 2 and 3. Comparative analysis of wild-type and mutants of lipases through RMSD analysis were well documented [33]. The time-dependent RMSD analysis reflects that the wild type and mutants of PML have less deviation as seen throughout the simulation. This implies that the 3D structures are relatively stable. The average and standard deviation of RMSD values of wild type and mutants of PML have been summarized in Table 3. Based on the average values of RMSD from Table 3, the order of stability was found to be (i) PML < P219A < P10A < E83R < P7A < P187A from ProSA study and (ii) PML < R91A < R163P < Q242P from RMSF study of PML. The RMSD analysis reflects that the

Table 2 List of *in silico* mutants of PML chosen for mutagenesis and their corresponding secondary structure

Study	PML#	Secondary structure*
PROSA	P187A	α-helix
	P219A	α-helix
RMSF	Q242P	loop
	R163P	loop
	R91A	α-helix

the data represented in the form: amino acid from wild type PML with its residue number followed by the amino acid chosen as the mutant

* the secondary structure where the mutants resides

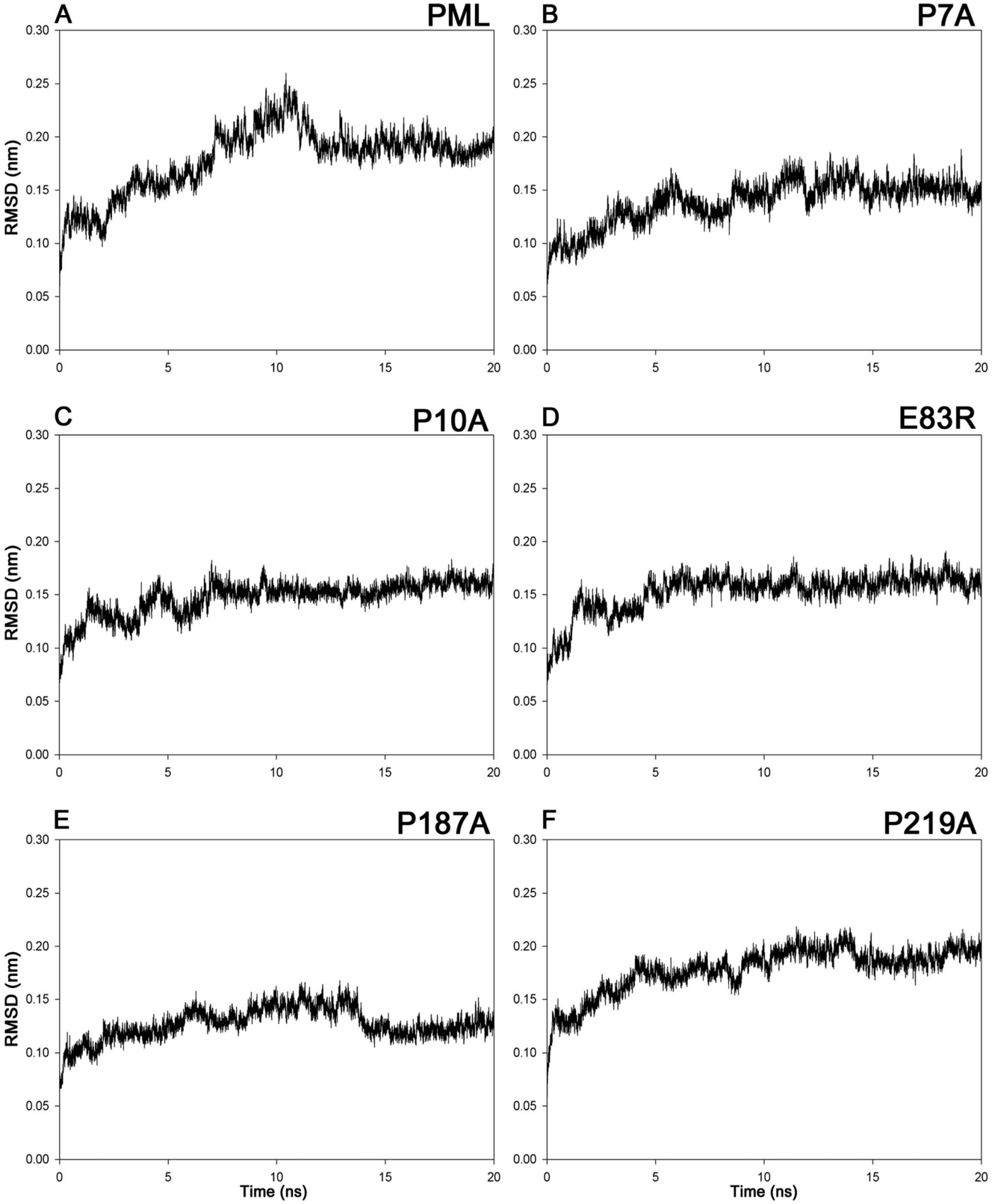

Fig. 2 The RMSD as a function of time of wild type and mutants of PML from ProSA study **a** PML (wild type), **b** Mutant P7A, **c** Mutant P10A, **d** Mutant E83R, **e** Mutant P187A, and **f** Mutant P219A

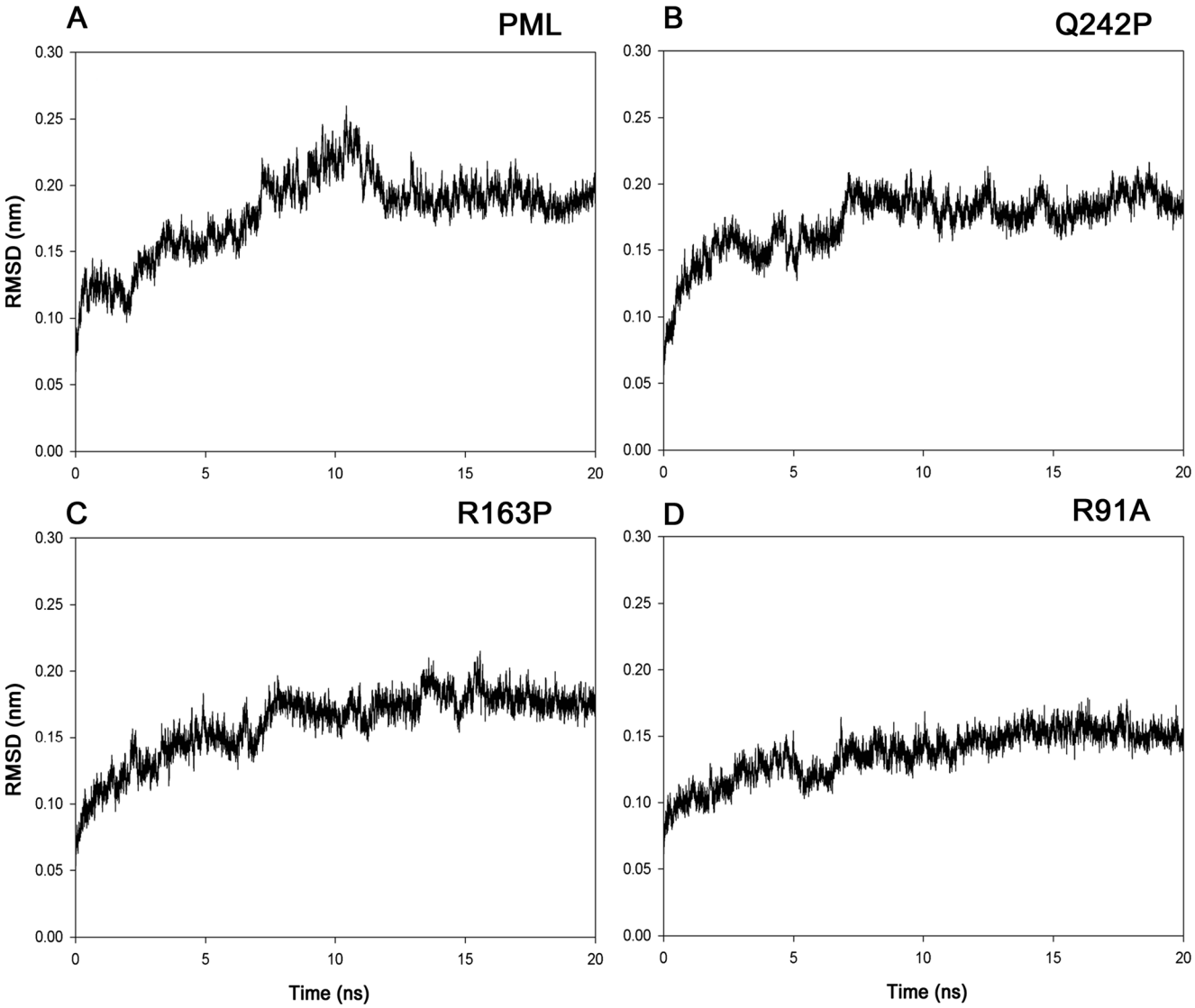

Fig. 3 The RMSD as a function of time of wild type and mutants of PML from RMSF study **a** PML (wild type), **b** Mutant Q242P, **c** Mutant R163P, and **d** Mutant R91A

Table 3 Summarized parameters of MD simulations for wild type and *in silico* mutants of PML

Method*	Variant	End to end distance (nm)	Radius of gyration (nm)	RMSD (nm)	RMSF (nm)	SASA (nm^2)
	PML	2.50±0.23	1.63±0.01	0.18±0.03	0.11±0.07	106.16±1.92
PROSA	P7A	2.08±0.33	1.63±0.01	0.14±0.02	0.11±0.06	104.66±2.03
	P10A	2.14±0.32	1.62±0.01	0.15±0.02	0.11±0.06	104.57±2.53
	E83R	1.78±0.22	1.63±0.01	0.15±0.02	0.10±0.05	105.12±1.97
	P187A	2.40±0.19	1.63±0.01	0.13±0.02	0.11±0.05	104.38±1.61
	P219A	1.90±0.29	1.62±0.01	0.18±0.02	0.11±0.06	103.41±1.91
RMSF	Q242P	2.23±0.31	1.62±0.01	0.14±0.02	0.11±0.05	103.60±2.22
	R163P	3.53±1.20	1.63±0.01	0.16±0.03	0.12±0.06	105.50±1.71
	R91A	4.06±1.01	1.62±0.01	0.17±0.02	0.11±0.07	104.13±2.35

* methodology implemented for the identification of the mutants

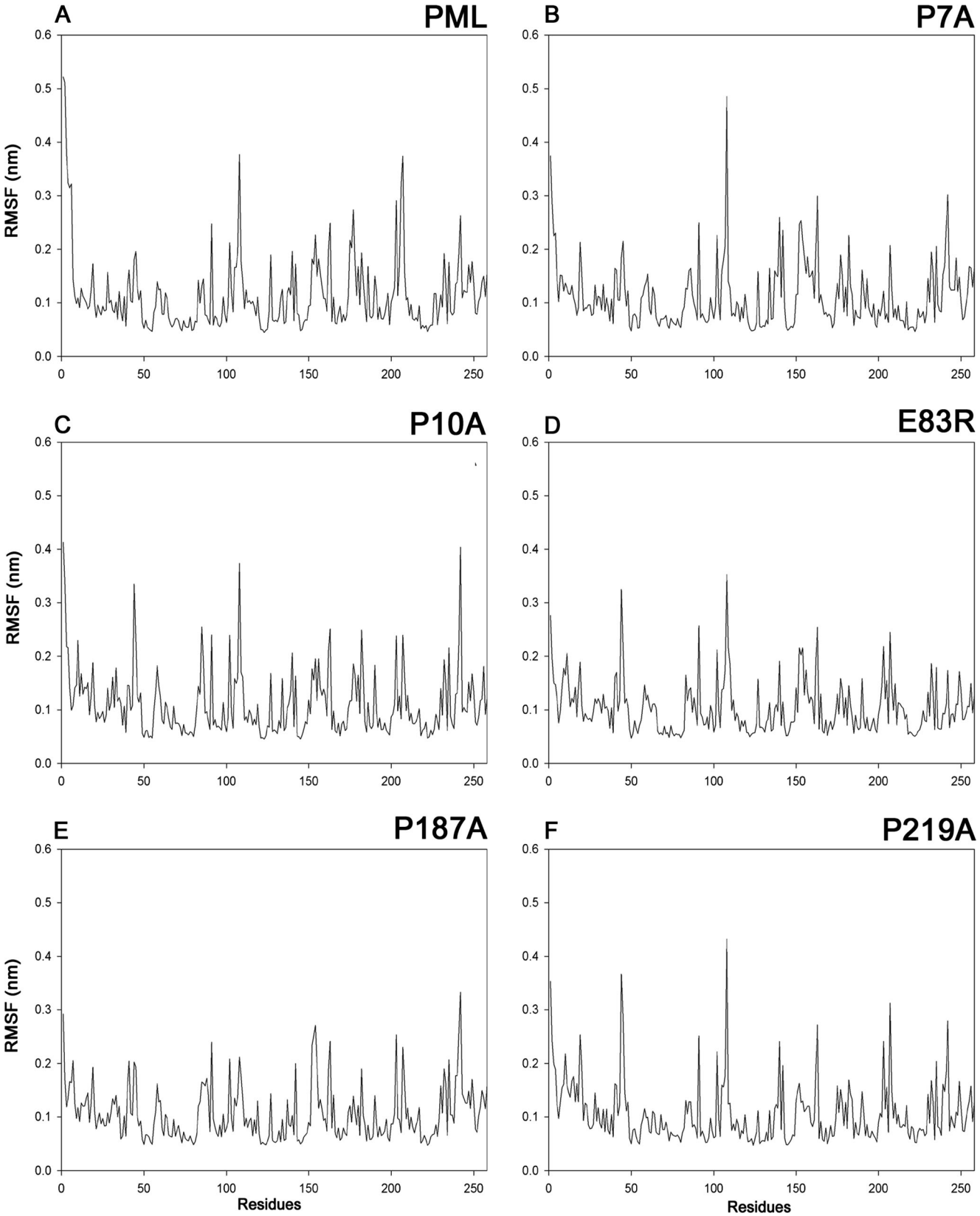

Fig. 4 RMSF of α-carbon atoms as a function of residue of wild type and mutants of PML from ProSA study **a** PML (wild type), **b** Mutant P7A, **c** Mutant P10A, **d** Mutant E83R, **e** Mutant P187A, and **f** Mutant P219A

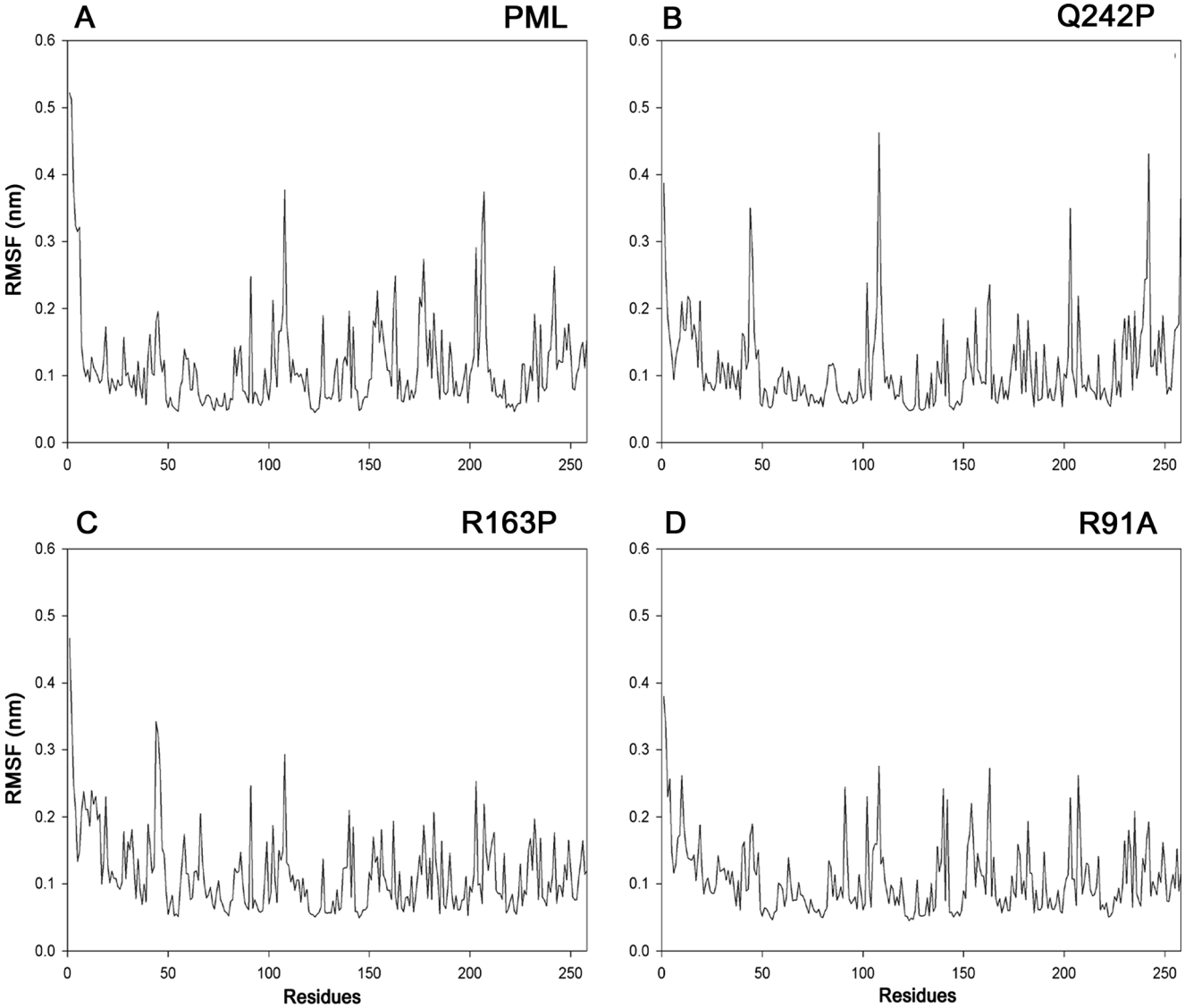

Fig. 5 RMSF of α-carbon atoms as a function of residue of wild type and mutants of PML from RMSF study **a** PML (wild type), **b** Mutant Q242P, **c** Mutant R163P, and **d** Mutant R91A

structural integrity of P219A, R91A, and R163P mutants is affected to a certain extent as compared to other mutants. Among ProSA mutants of PML, P187A mutant has comparatively better RMSD values which might be due to the stabilization of α-helix where Pro187 resides [33] (refer Fig. 8). Among mutants identified from RMSF studies, Q242P mutant was found comparatively more stable than other mutants. This is perhaps due to the stabilization of the loop where Glu242 resides and also the stabilization of the consecutive turn (refer to Fig. 9). The P7A mutant was also found to be more stable among the identified mutants.

Radius of gyration (Rg) The radius of gyration has been analyzed in a time-dependent manner to investigate the compactness of proteins [34]. The Rg trend of wild type and mutants of PML from ProSA and RMSF study has been presented in Supplementary Figs. 1 and 2 respectively. The radius of gyration reflects the packing of amino acids throughout the simulation thereby inferring stability and folding rate of PML. The wild type and identified mutants have a similar profile of Rg throughout the simulation. Table 3 reflects that the mutants P10A, P219A, R91A, and Q242P have better Rg profile than wild type PML. The Q242P mutant could be a better mutant in the context of Rg and RMSD analysis.

Root mean square fluctuation (RMSF) The local deformability of proteins has been analyzed through root mean square fluctuations of α-carbon atoms from MD simulations [35]. The RMSF plotted against the residues of wild type and mutants of PML from ProSA and RMSF study has been presented in Figs. 4 and 5 respectively. Appreciable difference of RMSF between wild type and mutants of PML is observed

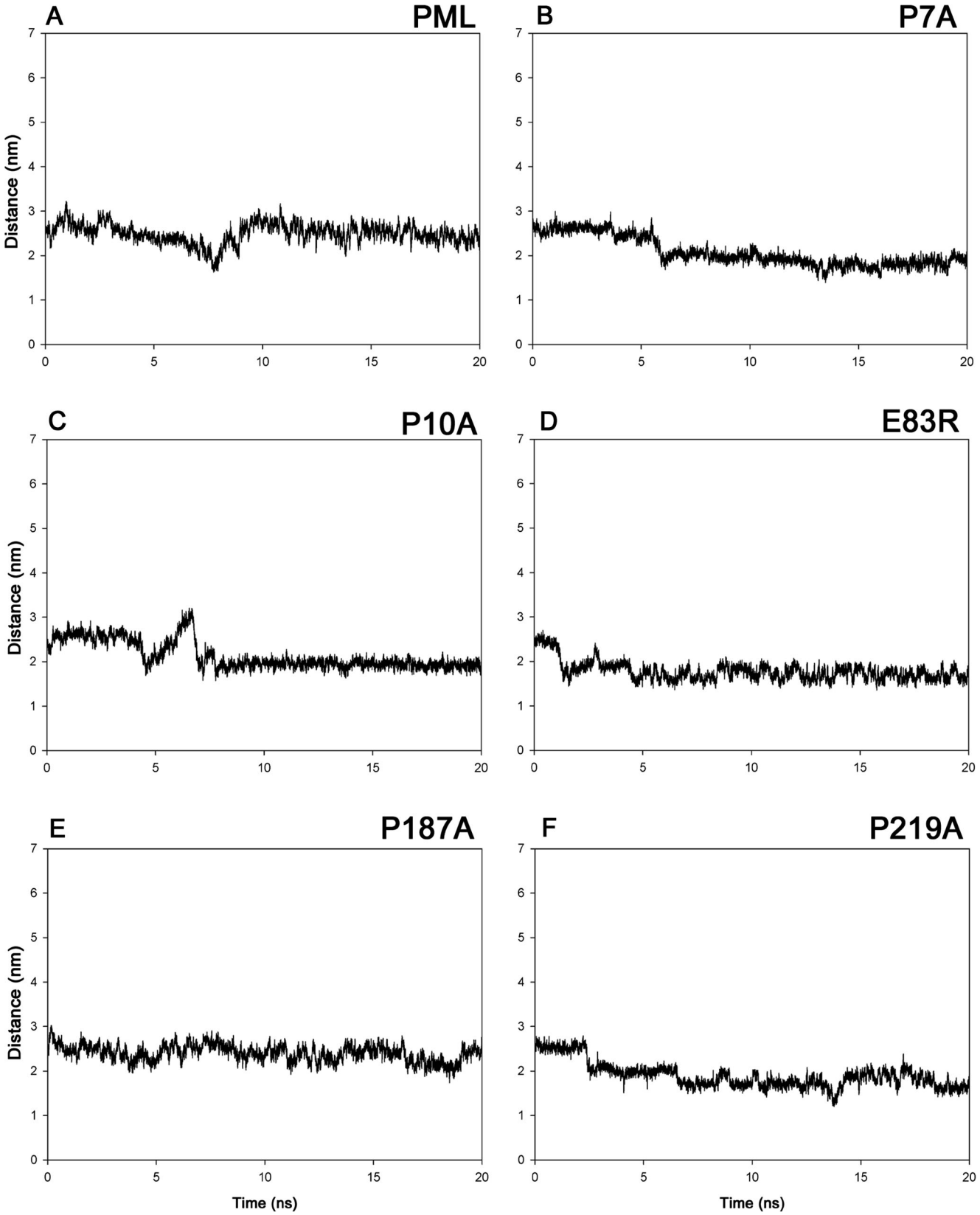

Fig. 6 The distance between first and last α-carbon atoms of wild type and mutants of PML from ProSA study **a** PML (wild type), **b** Mutant P7A, **c** Mutant P10A, **d** Mutant E83R, **e** Mutant P187A, and **f** Mutant P219A

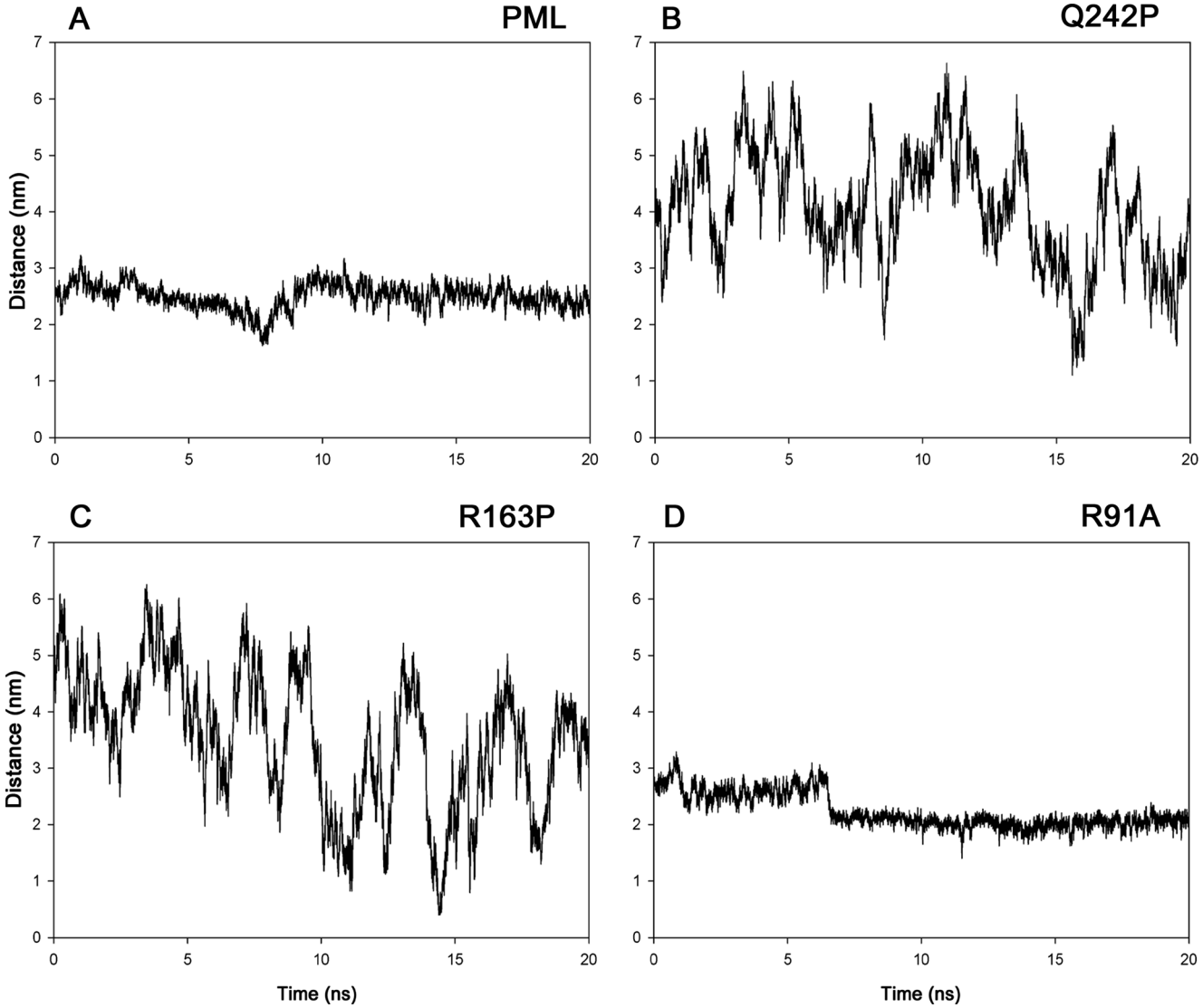

Fig. 7 The distance between first and last α-carbon atoms of wild type and mutants of PML from RMSF study **a** PML (wild type), **b** Mutant Q242P, **c** Mutant R163P, and **d** MutantR91A

at the N terminus (specifically the first 17 residues) which reflects the stabilization of the N terminus of the mutants. Appreciable difference at the mutation site is also observed at their respective regions. The P187A and R91A mutant show global reduction in the highly flexible regions while the average values of RMSF indicates the E83R mutant have considerable reduce in the RMSF values globally and the R163P mutant have considerable increase in the RMSF values globally.

Solvent accessible surface area (SASA) The surface accessibility of proteins has been analyzed to estimate the structural stability and served as utility for the comparative MD studies [36]. The trend of SASA analysis from Supplementary Figs. 3 and 4 reflects that the mutants and wild type of PML are similar and consistent with Rg analysis. The average values of SASA indicate that the mutants has considerably less hydrophobic area than wild type SXL2 (106.16±1.92 nm^2) notably P219A and Q242P mutants. It is evident from the SASA plots that the mutants had a comparatively steady SASA profile compared to the wild type. These point mutations make the mutants more robust than the wild type PML.

End to end chain distance between first and last α-carbon atoms The distance between first and last α-carbon atoms of wild type and mutants of PML from ProSA and RMSF study were analyzed throughout the simulation which would aid to understand the structural integrity of wild type and mutants of PML and have been presented in Figs. 6 and 7 respectively. Overall, a similar trend of end to end chain distance has been observed except for the mutants Q242P and R163P. Drastic changes have been observed in end to end chain distance in

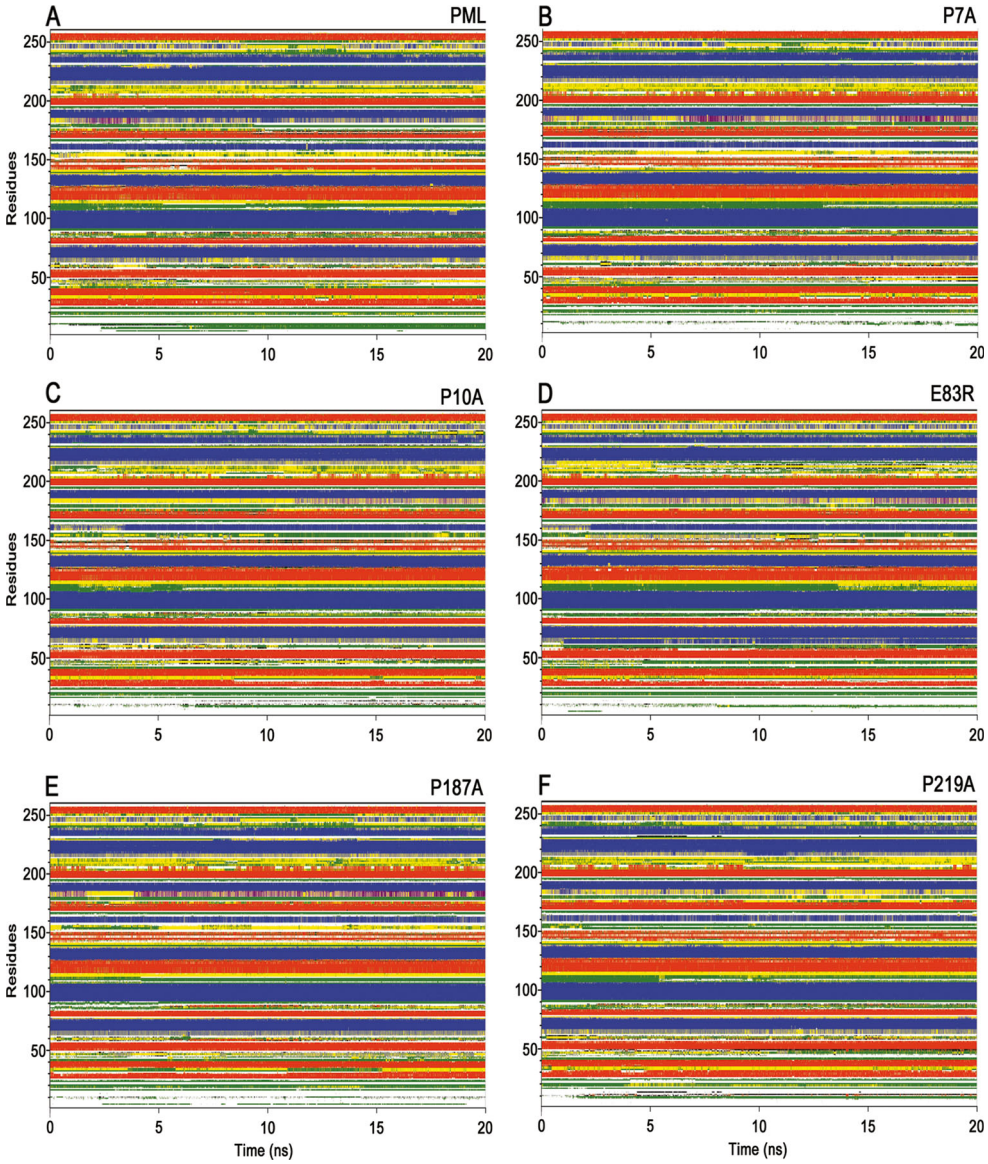

Fig. 8 The secondary structural analysis of wild type and mutants of PML from ProSA study **a** PML (wild type), **b** Mutant P7A, **c** Mutant P10A, **d** Mutant E83R, **e** Mutant P187A, and **f** Mutant P219A

mutants Q242P and R163P during the time course of simulation.

Analysis of secondary structure The DSSP utility aids to understand the structural stability of wild type and mutants through comparative MD studies [37]. The secondary structure analysis shows the structural variation of each residue of wild type and mutants of PML during the time course of simulation and has been presented in Figs. 8 and 9 respectively. The structural stabilization of the corresponding secondary structure with the identified mutants R91A, P187A, P219A, R163P, and Q242P were observed. Noticeable change in structural stabilization was not observed in the case of the mutants P7A, P10A, and E83R. Apart from structural stabilization of the corresponding α-helix, where the mutants P187A and P219A reside, they also stabilize the nearby secondary structure, turn and bend respectively. Meanwhile, reduced stabilization of the consecutive bend was observed in the case of the mutant R91A and R163P while the mutant R163P further destabilizes a nearby turn. Hence, it could be stated that these point mutations have a profound effect on the secondary structure of the region where the mutants reside.

The MD simulations of wild type and respective mutants of PML reflects that (i) the mutants E83R, P219A have better RMSD values, (ii) all the identified mutants have a similar trend of Rg as wild type while the mutants R91A, R163P have steadier equilibrium than wild type, (iii) RMSF analysis indicates that the mutants of PML

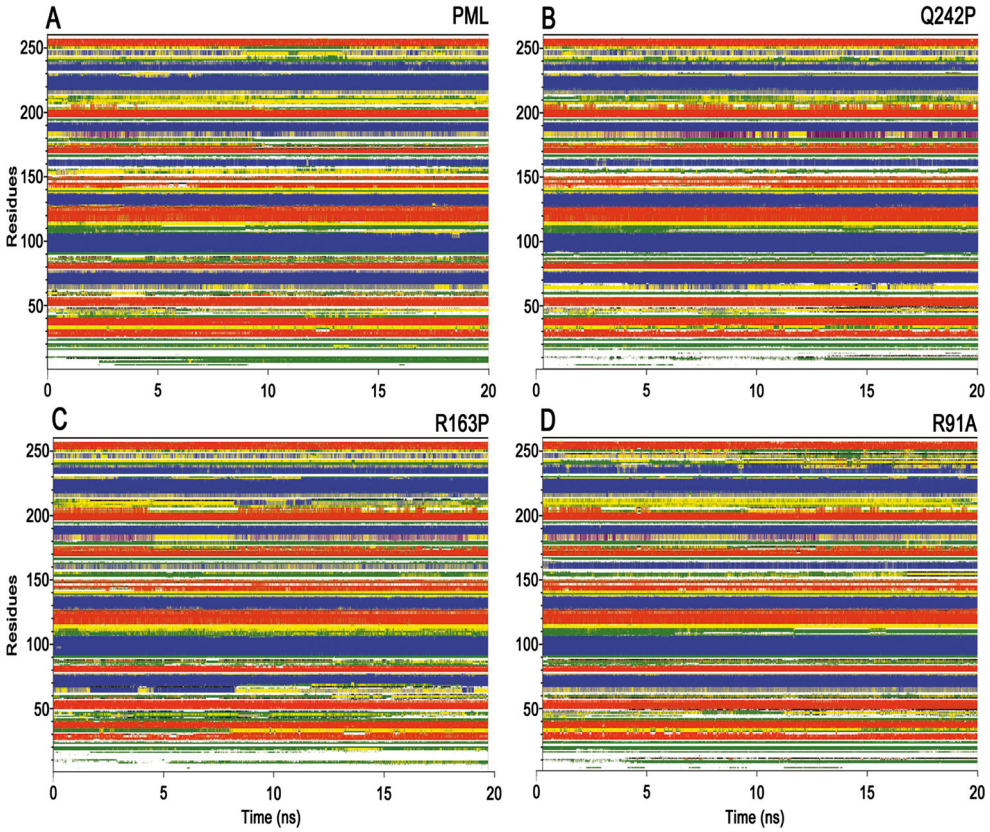

Fig. 9 The secondary structural analysis of wild type and mutants of PML from RMSF study **a** PML (wild type), **b** Mutant Q242P, **c** Mutant R163P, and **d** Mutant R91A

have comparative values with wild type while the mutants E83R, P219A have better RMSF values (iv) the mutants P219A, Q242P have lesser SASA values than wild type which reveals a decrease in solvent accessible hydrophobic area thereby the possibility of increase in compactness of hydrophobic core, (v) the mutants E83R and P219A have better 'end-to-end chain distance' values than wild type and (vi) the secondary structure variation analysis reveals that the mutants increased the stability of secondary structure where they reside, notably the mutants R91A (α-helix), P187A (α-helix), P219A (α-helix), R163P (loop). The discussed mutants of PML displayed increase in reduced flexibility, structural stability and lesser solvent exposed hydrophobic area which validates the *in silico* mutants. Apart from microscopic dynamics, macroscopic effects were also observed with the mutants P187A and P219A which would have correlation with the change in the biophysiochemical nature of PML. From the difference of RMSF with wild type PML, the mutant P187A has reduced molecular flexibility observed at N terminus with the first six residues, residues 176, 177 (bend 13), 206, and 207 (turn 13) (data not shown).

Overall, the current study attempted rational engineering of PML utilizing the structural bioinformatics approach which provides insights that could help to understand the structure of triacylglycerol lipases and also help to devise better strategies to design mutants to emulate their industrial applications.

Conclusions

Lipase from *Pseudomonas mendocina* (PML) was subjected to the rational bioinformatics approach to exploit its industrial applications. The current study engenders valuable insights to understand and identify new mutants of PML to improve its structural stability that might emulate its industrial potential. *In silico* characterization and mutational studies on PML identified structurally and functionally important residues. The predicted mutations of all possible sites using knowledge-based potentials from ProSA and RMSF data from MD identified mutagenesis hotspots. The identified *in silico* mutants were validated through comparative molecular dynamics with root mean square deviation (RMSD), radius of gyration (Rg), root mean square fluctuations (RMSF), solvent accessible surface area (SASA), end to end chain distance, and secondary structure analysis. Among the identified mutants, P187A and P219A mutants have better structural stability (RMSD), compactness (Rg, SASA, end to end chain distance), and reduced molecular flexibility (RMSF) than wild type PML. Apart from structural stabilization of the

corresponding α-helix, where the mutants P187A and P219A resides, they also stabilize the nearby secondary structure, turn and bend respectively. The mutants P187A and P219A have reduced molecular flexibility and improved compactness compared to wild type PML as well as the stabilization of local dynamics which underlies its improved structural stability. MD simulations also reveal the correlation between microscopic dynamics and macroscopic properties in PML. These predicted *in silico* mutants can be taken further toward *in vitro* validations and their suitability in industrial applications.

References

1. Hasan F, Shah AA, Hameed A (2006) Industrial applications of microbial lipases. Enzym Microb Technol 39:235–251
2. Guncheva M, Zhiryakova D (2011) Catalytic properties and potential applications of Bacillus lipases. J Mol Catal B Enzym 68:1–21
3. Goswami D, Basu JK, De S (2013) Lipase applications in oil hydrolysis with a case study on castor oil: a review. Crit Rev Biotechnol 33: 81–96
4. Kapoor M, Gupta MN (2012) Lipase promiscuity and its biochemical applications. Process Biochem 47:555–569
5. Narwal SK, Gupta R (2013) Biodiesel production by transesterification using immobilized lipase. Biotechnol Lett 35:479–490
6. Naik S, Basu A, Saikia R, Madan B, Paul P, Chaterjee R, Brask J, Svendsen A (2010) Lipases for use in industrial biocatalysis: specificity of selected structural groups of lipases. J Mol Catal B Enzym 65:18–23
7. Nestl BM, Nebel BA, Hauer B (2011) Recent progress in industrial biocatalysis. Curr Opin Chem Biol 15:187–193
8. Haki GD, Rakshit SK (2003) Developments in industrially important thermostable enzymes: a review. Bioresour Technol 89:17–34
9. Illanes A (1999) Stability of biocatalysts. Electron J Biotechnol 21:7–15
10. Shu ZY, Jiang H, Lin RF, Jiang YM, Lin L, Huang JZ (2010) Technical methods to improve yield, activity and stability in the development of microbial lipases. J Mol Catal B Enzym 62:1–8
11. Looger LL, Dwyer MA, Smith JJ, Hellinga HW (2003) Computational design of receptor and sensor proteins with novel functions. Nature 423:185–190
12. Benjamin S, Pandey A (1998) Candida rugosa lipases: molecular biology and versatility in biotechnology. Yeast 14:1069–1087
13. Jaeger KE, Eggert T (2002) Lipases for biotechnology. Curr Opin Biotechnol 13:390–397
14. Ravi B, Banerjee U, Mehrotra S, Mehrotra R (2013) Engineering lipases for enhanced catalysis. Curr Chem Biol 7:114–120
15. Arendse L, Blundell TL, Blackburn J (2013) Combining in silico protein stability calculations with structure-function relationships to explore the effect of polymorphic variation on cytochrome P450 drug metabolism. Curr Drug Metab 14:745–763
16. Bora L, Gohain D, Das R (2013) Recent advances in production and biotechnological applications of thermostable and alkaline bacterial lipases. J Chem Technol Biotechnol 88:1959–1970
17. Cherif S, Mnif S, Hadrich F, Abdelkafi S, Sayadi S (2011) A newly high alkaline lipase: an ideal choice for application in detergent formulations. Lipids Health Dis 10:221
18. Schomburg I, Chang A, Placzek S, Söhngen C, Rother M, Lang M, Munaretto C, Ulas S, Stelzer M, Grote A, Scheer M, Schomburg D (2013) BRENDA in 2013: integrated reactions, kinetic data, enzyme function data, improved disease classification: new options and contents in BRENDA. Nucleic Acids Res 41(Database issue):764–772
19. Lailaja VP, Chandrasekaran M (2013) Detergent compatible alkaline lipase produced by marine Bacillus smithii BTMS 11. World J Microbiol Biotechnol 29:1349–1360
20. Li XL, Shi Y, Zhang WH, Dai YJ, Zhang HT, Wang Y, Lu FP (2014) A high-detergent-performance, cold-adapted lipase from Pseudomonas stutzeri > PS59 suitable for detergent formulation. J Mol Catal B, Enzym
21. Wang YX, Srivastava KC, Shen GJ, Wang HY (1995) Thermostable alkaline lipase from a newly isolated thermophilic Bacillus, strain A30-1 (ATCC 53841). J Ferment Bioeng 79:433–438
22. Boston M, Requadt C, Danko S, Jarnagin A, Ashizawa E, Wu S, Poulose AJ, Bott R (1997) Structure and function of engineered Pseudomonas mendocina lipase. Methods Enzymol 284:298–317
23. Sibille N, Favier A, Azuaga AI, Ganshaw G, Bott R, Bonvin AM, Boelens R, van Nuland NA (2006) Comparative NMR study on the impact of point mutations on protein stability of Pseudomonas mendocina lipase. Protein Sci 15:1915–1927
24. Sippl MJ (1993) Recognition of errors in three-dimensional structures of proteins. Proteins Struct Funct Genet 17:355–362
25. Parameswaran S, Throat AA, Patra S (2010) Deciphering role of amino acids for the stability of Staphylococcus aureus lipase (SAL3). Interdisc Sci 2:27127–27129
26. Hess B (2008) P-LINCS: a parallel linear constraint solver for molecular simulation. J Chem Theory Comput 4:116–122
27. Pronk S, Páll S, Schulz R, Larsson P, Bjelkmar P, Apostolov R, Shirts MR, Smith JC, Kasson PM, van der Spoel D, Hess B, Lindahl E (2013) GROMACS 4.5: a high-throughput and highly parallel open source molecular simulation toolkit. Bioinformatics 29:845–854
28. Van Der Spoel D, Lindahl E, Hess B, Groenhof G, Mark AE, Berendsen HJ (2005) GROMACS: fast, flexible, and free. J Comput Chem 26:1701–1718
29. Kabsch W, Sander C (1983) Dictionary of protein secondary structure: pattern recognition of hydrogen-bonded and geometrical features. Biopolymers 22:2577–2637
30. Chou PY, Fasman GD (1974) Conformational parameters for amino acids in helical, β-sheet, and random coil regions calculated from proteins. Biochem 13:211–222
31. Acharya P, Rajakumara E, Sankaranarayanan R, Rao NM (2004) Structural Basis of Selection and Thermostability of Laboratory Evolved *Bacillus subtilis* Lipase. J Mol Biol 341:1271–1281
32. Frenken LG, Egmond MR, Batenburg AM, Verrips CT (1993) Pseudomonas glumae lipase: increased proteolytic stabifity by protein engineering. Protein Eng 6:637–642
33. Khurana J, Singh R, Kaur J (2011) Engineering of Bacillus lipase by directed evolution for enhanced thermal stability: effect of isoleucine to threonine mutation at protein surface. Mol Biol Rep 38:2919–2926
34. Pikkemaat MG, Linssen AB, Berendsen HJ, Janssen DB (2002) Molecular dynamics simulations as a tool for improving protein stability. Protein Eng 15:185–192
35. Hou T, Yu R (2007) Molecular dynamics and free energy studies on the wild-type and double mutant HIV-1 protease complexed with amprenavir and two amprenavir-related inhibitors: mechanism for binding and drug resistance. J Med Chem 50:1177–1188
36. Yin S, Ding F, Dokholyan NV (2007) Modeling backbone flexibility improves protein stability estimation. Structure 15:1567–1576
37. Hirschberger T, Stork M, Schropp B, Winklhofer KF, Tatzelt J, Tavan P (2006) Structural instability of the prion protein upon M205S/R mutations revealed by molecular dynamics simulations. Biophys J 90(11):3908–3918